Proc. Int. Symposium on Neutron Optics and Related Research Facilities, Kumatori, 1996
J. Phys. Soc. Jpn. **65** (1996) Suppl. A pp. 249–251

Upgrade of Neutron Guides with Use of Supermirrors

Klaus Al Usta, *Kalyana N'Guy, *Alain Menelle, and François Samuel

CILAS, Compagnie Industrielle des Lasers, Route de Nozay, 91460 Marcoussis, FRANCE
**Laboratoire Léon Brillouin (CEA-CNRS), CEA-Saclay, 91191 Gif-sur-Yvette Cedex, FRANCE*

(Received 11 March 1996; accepted 4 April 1996)

Recent industrial developments of neutron supermirrors enable now the building of large surface elements, with an apparent critical angle double of the natural nickel, and a reflectivity of more than 90% on the extension of the total reflection plateau. Neutron guide G3-bis, and the curved part of the guide G2 on the Orphée reactor at Saclay (France) have been recently upgraded taking profit of this new technology. Thermal neutron flux and wavelength intensity distributions available at the end of guides G3-bis and G2 before and after this modification have been measured. An increase of flux of 69% on G3-bis, and 21% on G2 have been obtained.

KEYWORDS: Neutron guide , supermirror

§.1. Introduction

Recent developments in supermirror coatings allow the manufacturing of neutron mirrors with high reflectivity (> 90%) on large surfaces and with an effective critical angle of twice the critical angle of natural nickel. In August 1994, the neutron guide G3-bis at the Orphée reactor of the Laboratoire Léon Brillouin (LLB) in Saclay (France) was upgraded using supermirrors. A few months later, in February 1995, the curved part of the guide G2 installed on the same reactor was also upgraded using supermirrors. We report in this paper intensity measurements made on these two guides before and after the modifications.

At LLB, six cold neutron beams are used to feed a large experimental hall through six horizontally curved neutron guides and three neutron guide benders.[1] The transmission of thermal neutrons in a curved guide is determined by three quantities: the critical angle $\theta_c = \gamma_c \lambda$ of the coating material, the width W of the guide and the radius of curvature R. Here λ is the neutron wavelength; the quantity γ_c depends on the coating material, e.g. $\gamma_c = 0.117°/\text{Å}$ for ^{58}Ni. At each guide corresponds a characteristic wavelength[2] $\lambda_c = \sqrt{2W/\gamma_c^2 R}$. Transmission of wavelength shorter than λ_c will be small.

A need for shorter wavelengths is expressed in more and more experiments done on the reflectometers and small angle machines of this experimental hall. To fulfill this demand, a decrease of λ_c of the corresponding guides is necessary. The use of supermirrors with high γ_c enables to obtain this result without geometrical modification of the whole setup of the guide. This is very interesting in an existing experimental hall as is the case at LLB. In summer 1994, the elements of the neutron guide bender G3-bis (coated with ^{58}Ni), which feeds the time-of-flight reflectometer EROS, were changed by supermirrors coated elements. In February 1995, the same operation was done on the curved part of the guide G2 (coated with ^{nat}Ni) which feeds the small angle scattering spectrometer PAXY.

§.2. Description of guides and supermirrors

G3-bis is a bender installed on the guide G3.[3] The first part of G3 has a length of 13.5*m* and a section of 150*mm* in height by 25*mm* in width. The radius of curvature is 4167*m*. Coated with ^{nat}Ni this curved part shows a characteristic wavelength of 2.0Å. The neutron beam is then split vertically into two beams of section 50×25*mm*^{2} each. The upper part (main guide G3) continues on a length of 26*m*. The lower part of the neutron beam is deviated from the main guide using a curved multichannel guide (made of five channels of 4.6*mm* in width). Its length is 3*m*. It is followed by a straight guide element of 6*m* length. Together, these parts form the guide G3-bis. Coated with ^{58}Ni it has a characteristic wavelength λ_c of 6.6Å. G2 has a curved length of 23*m* with a section of 150×25*mm*^{2}. The radius of curvature is 1042*m*. Coated with ^{nat}Ni, its characteristic wavelength is 4.0Å. It is followed by a straight part of 16*m* length.

Table.1. Thermal neutron flux, characteristic wavelengths λ_c and transmissions for G2, G3 and G3-bis before and after modification of the guides.

	G3 Shutter level	G3 end	End of G3-bis (^{58}Ni)	End of G3-bis (supermirrors)
Neutron flux (n.cm^{-2}.s^{-1})	2.1×10^9	1.7×10^9	0.7×10^9	1.1×10^9
λ_c (Å)		2.0	6.6	4.1
Transmission		81%	35%	52%
	G2 beginning		**End of G2 (^{nat}Ni)**	**End of G2 (supermirrors)**
Neutron flux (n.cm^{-2}.s^{-1})	1.7×10^9		1.2×10^9	1.4×10^9
λ_c (Å)			4.0	2.0
Transmission			70%	82%

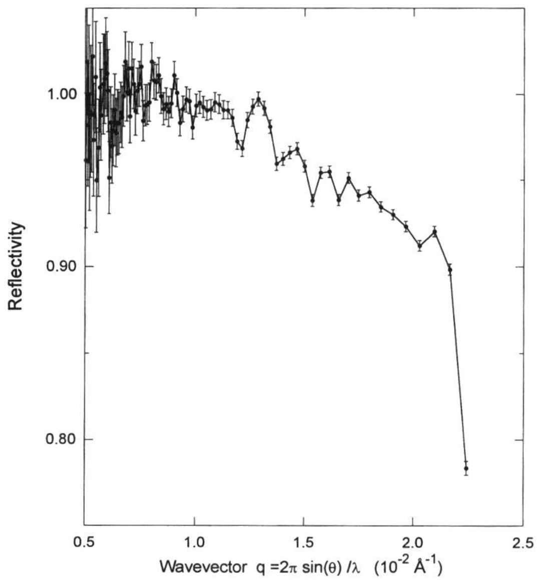

Fig. 1. Measured reflectivity for one of the supermirrors used for G3-bis.

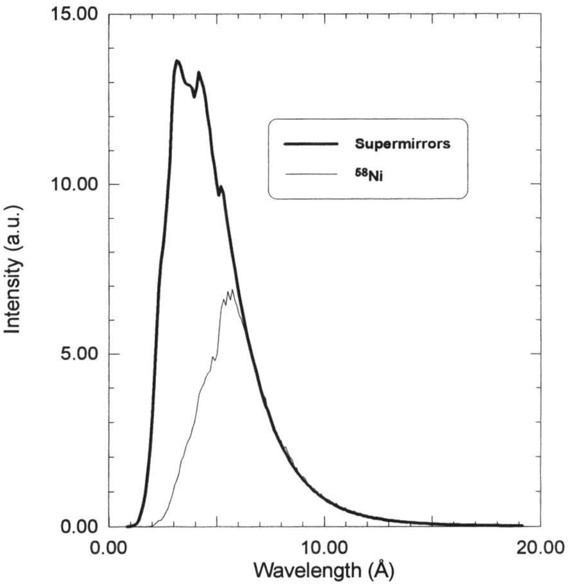

Fig. 2. Intensity distribution on EROS at the end of G3-bis.

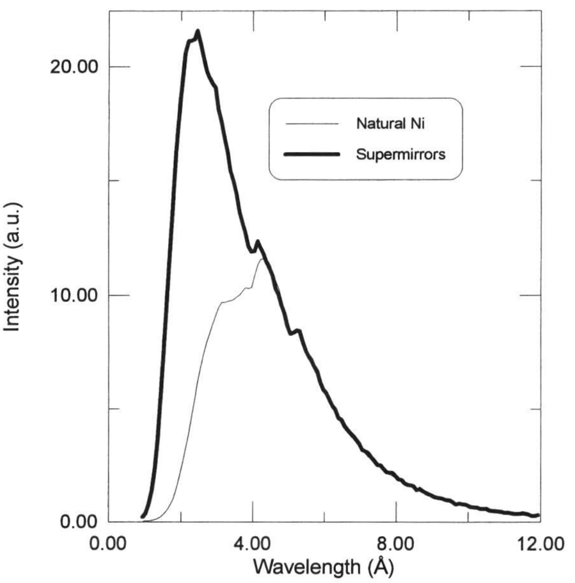

Fig. 3. Intensity distribution on PAXY at the end of G2.

The supermirror coatings were produced by CILAS (Compagnie Industrielle de Laser) who also manufactured the guide elements. The mirror coatings are made by magnetron sputtering of alternate $Ni_{(1-x)}C_x$ (with $x \approx 0.1$) and Ti layers of increasing thickness. During the fabrication of the guide G3-bis, the quality of the supermirror coatings was controlled on the EROS reflectometer using a multireflection technique.[4] A typical reflectivity curve as a function of wavevector is represented on Fig. 1. The total external reflection plateau of $Ni_{(1-x)}C_x$ that extends up to a wavevector of 0.011Å^{-1} is followed by an extended reflection range where the reflectivity decreases slowly from 99.9% at 0.011Å^{-1} to 90% at a wavevector of 0.021Å^{-1}. This wavevector corresponds to an effective critical angle of γ_c=0.19°/Å. For all tested mirrors the variations of γ_c, and of the mirror reflectivity, was within ± 3%.

§.3. Gold foils activation measurements

The efficiency of the modifications of the guides has been compared first by using flux measurements at the end of the guides G2, G3 and G3-bis, at the shutter location of G3 (beginning of G3-bis), and at the beginning of G2. They have been done by activation of thin gold foils of 0.1*mm*. A cross section of 98 barns was used for the determination of the flux, and they were normalized to a reactor power of 14MW. No correction was applied for the variation of wavelength distribution. The results are presented in Table 1. The most important fact is the 50% and 16% increase of flux available at the end of G3-bis and G2 respectively. The second interesting feature of this comparison is that, despite a characteristic wavelength of 4.1Å, which is much larger than the 2Å of the main guide, we obtain a transmission as large as 52% for G3-bis. The transmission of G2 is also increased from 70% to 82%, and is now comparable to the transmission of G3 (81%) which possess a smaller characteristic wavelength.

§.4. Intensity distribution measurements

Up to this point, we have not taken into account the variation of the neutron flux with wavelength. We have measured the wavelength distribution using the time-of-flight technique. The measured intensity distributions, before and after the upgrade, are reported on Fig. 3. Between the old guides and the new ones, the maximum available intensities on the instruments have been multiplied by a factor 2 and the corresponding wavelength shifted from 5.7Å, to 3.1Å, on G3-bis, and from 4.2Å, to 2.9Å, on G2. This is a direct effect of the supermirror large critical angle that enables a better transmission of the short wavelengths

Intensity distribution measurements have been performed with an angular resolution of 0.3° for G3-bis, and 0.15° for G2. However, for wavelengths larger than 3Å, the divergence of the beam at the end of the guides is much larger than the divergence used in the intensity distribution measurements. Therefore, we do not measure the correct variation of the transmitted flux at large wavelength, since the flux increase is obtained mainly by an increase of the divergence. To take into account for this effect, a correction is applied to the measured wavelength distribution to obtain the effective neutron-flux distribution within the guide. This distribution is then used to calculate the gold absorption cross section necessary to extract the exact neutron flux from the gold foil activation measurements. For G3-bis, we obtained 1.66×10^8 $n.c.m^{-2}.s^{-1}$ with ^{58}Ni and 2.8×10^8 $n.c.m^{-2}.s^{-1}$ with supermirrors; for G2: 2.33×10^8 $n.c.m^{-2}.s^{-1}$ with ^{nat}Ni, 2.83×10^8 $n.c.m^{-2}.s^{-1}$ with supermirrors. Normalized corrected intensity distributions to these numbers are represented on Fig. 4 and 5. The characteristic features are now the following for G3-bis: a 69% increase of the total flux available, a 51% improvement of the maximum intensity , and a shift from 6.1Å, to 5.4Å, in this maximum of the transmitted neutron flux. On G2, we obtain a 21% increase of the total flux available, a 5% improvement of the maximum intensity, and a shift from 4.5Å, to 2.9Å, in this maximum of the transmitted neutron flux.

§.5. Conclusion

To conclude, our results demonstrate the advantage of the use of supermirrors for old and new neutron beam installations. By comparison with gold foil activation measurements, and time of flight intensity distribution measurements, we show that the enhancement of intensity obtained on instruments installed on guides is very dependent on its resolution, and it can be larger than simply the gain in flux. In order to benefit from this new technology, other neutron guides at the Orphée reactor, feeding selected instruments, will certainly be upgraded in a near future.

1) M.C. Bellissent-Funel, *Neutron News* 3.1 (1992) 7-15.
2) B. Farnoux, B. Hennion and J. Fagot, *Neutron Inelastic Scattering*, Conf. Proc. IAEA, Vienna 2 (1968) 353-80.
3) B. Ballot, F. Samuel and B. Farnoux, *SPIE Proc.* 1738 (1992) 159-165.
4) B. Ballot, A. Menelle, F. Samuel, K. Al Usta and B. Farnoux, *Physica* B 198 (1994) 213-216.

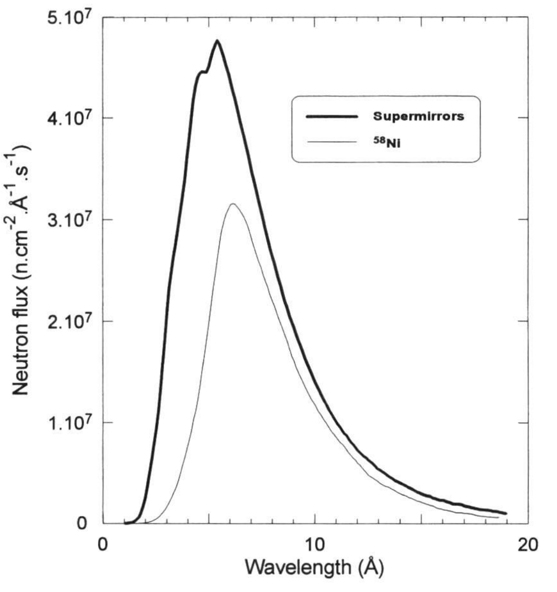

Fig. 4. Flux distribution at the end of G3-bis.

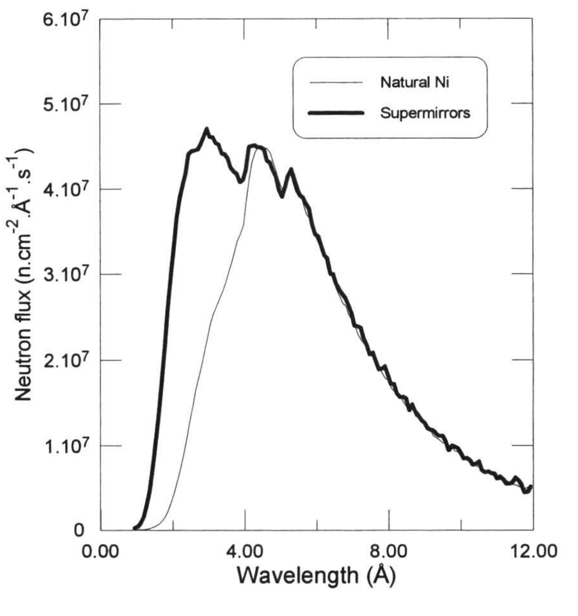

Fig. 5. Flux distribution at the end of G2.